NJNU-TH-06-24

Branching Ratio and CP Asymmetry of $B_s \to \rho(\omega)K$ Decays in the Perturbative QCD Approach

Zhen-jun Xiao , Xin-fen Chen and Dong-qin Guo

Department of Physics and Institute of Theoretical Physics,
Nanjing Normal University, Nanjing, Jiangsu 210097, P.R.China

(Dated: February 2, 2008)

arXiv:hep-ph/0608222v1 20 Aug 2006

Abstract

In this paper, we calculate the branching ratios and CP-violating asymmetries for $B_s \to \rho^{\pm}K^{\mp}$, $B_s \to \rho^0\overline{K}^0$ and $B_s \to \omega\overline{K}^0$ decays in the perturbative QCD (pQCD) factorization approach. The theoretical predictions for the CP averaged branching ratios of the considered decays are: $Br(B_s \to \rho^{\pm}K^{\mp}) \approx 24.7 \times 10^{-6}$, $Br(B_s \to \rho^0\overline{K}^0) \approx 1.2 \times 10^{-7}$ and $Br(B_s \to \omega\overline{K}^0) \approx 1.7 \times 10^{-7}$; and we also predict very large direct CP-violating asymmetries for the latter two decay modes: $A_{CP}^{dir}(\rho^{\pm}K^{\mp}) \approx -12\%$, $A_{CP}^{dir}(\rho^0\overline{K}^0) \approx -92\%$, $A_{CP}^{dir}(\omega^0\overline{K}^0) \approx 81\%$, $A_{CP}^{mix}(\rho^0\overline{K}^0) \approx -36\%$, and $A_{CP}^{mix}(\omega^0\overline{K}^0) \approx -40\%$, which can be tested in the forthcoming LHC-b experiments.

PACS numbers: 13.25.Hw, 12.38.Bx, 14.40.Nd

I. INTRODUCTION

The charmless B meson decay is a good place to test the Standard Model (SM), study CP violation and look for signal or evidence of possible new physics beyond the SM. Since 1999, many such decay modes have been observed in the B factory experiments. In the forthcoming Large Hadron Collider beauty (LHC-b) experiments, a large number of heavier B_s and B_c mesons together with light $B_{u,d}$ mesons will be produced [1]. The study about the charmless decays of B_s meson therefore is therefore becoming more interesting then ever before [2].

By employing the generalized facterization approach[3, 4, 5] or the QCD factorization (QCDF) approach [6], about 40 $B_s \to h_1 h_2$ (h_i stand for light pseudo-scalar or vector mesons) decay modes have been studied in the framework of SM [7, 8, 9, 10] or in some new physics models beyond the SM [11]. In Refs. [12, 13, 14, 15, 16], the branching ratios and CP violating asymmetries of $B_s \to \pi^+\pi^-, \pi\rho$, πK, $\rho(\omega)K^*$ and $\pi\eta^{(\prime)}$ decays have been calculated by employing the perturbative QCD (pQCD) factorization approach [17, 18]. Motivated by the expected successes in LHC-b experiments and other hadronic B meson experiments, we here continue to investigate more charmless B_s decays in pQCD factorization approach.

In this paper, we will study the $B_s \to \rho^\pm K^\mp$, $\rho^0\overline{K}^0$ and $\omega\overline{K}^0$ decays in the pQCD approach. In principle, the physics for the B_s two-body hadronic decays is very similar to that for the B_d meson except that the spectator d quark is replaced by the s quark. Theoretically, the three decays have been studied before in the naive or generalized factorization approach, as well as in the QCD factorization approach[9, 10]:

For $B_s \to \rho(\omega)K$ decays, the B_s meson is heavy, setting at rest and decaying into two light mesons (i.e. $\rho(\omega)$ and K) with large momenta. Therefore the light final state mesons are moving very fast in the rest frame of B_s meson. In this case, the short distance hard process dominates the decay amplitude. We assume that the soft final state interaction is not important for such decays, since there is not enough time for light mesons to exchange soft gluons. Therefore, it makes the pQCD reliable in calculating the $B_s \to \rho(\omega)K$ decays. With the Sudakov resummation, we can include the leading double logarithms for all loop diagrams, in association with the soft contribution. Unlike the usual factorization approach, the hard part of the pQCD approach consists of six quarks rather than four. We thus call it six-quark operators or six-quark effective theory. Applying the six-quark effective theory to B_s meson decays, we need meson wave functions for the hadronization of quarks into mesons. All the collinear dynamics are included in the meson wave functions.

This paper is organized as follows. In Sec. II, we give a brief review for the pQCD factorization approach. In Sec. III, we calculate analytically the related Feynman diagrams and present the decay amplitudes for the studied decay modes. In Sec. IV, we show the numerical results for the branching ratios and CP asymmetries of $B_s \to \rho(\omega)K$ decays and comparing them with the results obtained in the QCDF approach. The summary and some discussions are included in the final section.

II. THEORETICAL FRAMEWORK

The three scale pQCD factorization approach has been developed and applied in the non-leptonic $B_{(s)}$ meson decays for some time. In this approach, the decay amplitude is separated into soft (Φ), hard(H), and harder(C) dynamics characterized by different energy scales (t, m_b, M_W) . It is conceptually written as the convolution:

$$\mathcal{A}(B_{(s)} \to M_1 M_2) \sim \int d^4k_1 d^4k_2 d^4k_3 \ \mathrm{Tr}\left[C(t)\Phi_{B_{(s)}}(k_1)\Phi_{M_1}(k_2)\Phi_{M_2}(k_3)H(k_1,k_2,k_3,t)\right], \quad (1)$$

where k_i's are momenta of light quarks included in each mesons, and Tr denotes the trace over Dirac and color indices. The harder dynamic involves the four quark operators described by the Wilson coefficient $C(t)$. It results from the radiative corrections to the four quark operators at short distance. In the above convolution, $C(t)$ includes the harder dynamics at larger scale than $M_{B_{(s)}}$ scale and describes the evolution of local 4-Fermi operators from m_W (the W boson mass) down to $t \sim \mathcal{O}(\sqrt{\bar{\Lambda} M_{B_{(s)}}})$ scale, where $\bar{\Lambda} \equiv M_{B_{(s)}} - m_b$. The function $H(k_1, k_2, k_3, t)$ describes the four quark operator and the spectator quark connected by a hard gluon whose scale is at the order of $M_{B_{(s)}}$,so this hard part H can be perturbatively calculated.The hard and harder dynamics together make an effective six-quark interaction. The soft dynamic is factorized into the meson wave function Φ_M ,which describes hadronization of the quark and anti-quark pair into the meson M. While the function H depends on the processes considered, the wave function Φ_M is independent of the specific processes. Using the wave functions determined from other well measured processes, one can make quantitative predictions here.

For the B_s meson decays, since the b quark is rather heavy we consider the B_s meson at rest for simplicity. It is convenient to use light-cone coordinate $(p^+, p^-, \mathbf{p}_T)$ to describe the meson's momenta. The B_s meson and the two final state meson momenta can be written as

$$P_{B_s} = \frac{M_{B_s}}{\sqrt{2}}(1, 1, \mathbf{0}_T), \quad P_{\rho(\omega)} = \frac{M_{B_s}}{\sqrt{2}}(1, r^2_{\rho(\omega)}, \mathbf{0}_T), \quad P_k = \frac{M_{B_s}}{\sqrt{2}}(0, 1 - r^2_{\rho(\omega)}, \mathbf{0}_T), \quad (2)$$

respectively, where $r_\rho = m_\rho / M_{B_s}$; the light pseudoscalar meson masses have been neglected.

For the $B_s \to \rho(\omega)K$ decays considered here, only the $\rho(\omega)$ meson's longitudinal part contributes to the decays, its polar vector is $\epsilon_L = \frac{M_{B_s}}{\sqrt{2}M_{\rho(\omega)}}(1, -r^2_{\rho(\omega)}, \mathbf{0_T})$. Putting the light (anti-) quark momenta in B_s, $\rho(\omega)$ and k mesons as k_1, k_2, and k_3, respectively, we can choose

$$k_1 = (x_1 P_1^+, 0, \mathbf{k}_{1T}), \quad k_2 = (x_2 P_2^+, 0, \mathbf{k}_{2T}), \quad k_3 = (0, x_3 P_3^-, \mathbf{k}_{3T}). \quad (3)$$

Unlike the QCD factorization approach,we don't neglect the transverse momentum k_T in the above expressions, by which to avoid the endpoint singularity.Then, the integration over k_1^-, k_2^-, and k_3^+ in eq.(1) will lead to

$$\mathcal{A}(B_s \to \rho(\omega)k) \sim \int dx_1 dx_2 dx_3 b_1 db_1 b_2 db_2 b_3 db_3 \\ \mathrm{Tr}\left[C(t)\Phi_{B_s}(x_1, b_1)\Phi_{\rho(\omega)}(x_2, b_2)\Phi_k(x_3, b_3)H(x_i, b_i, t)S_t(x_i)\, e^{-S(t)}\right], \quad (4)$$

where b_i is the conjugate space coordinate of k_{iT}, and t is the largest energy scale in function $H(x_i, b_i, t)$, as a function in terms of x_i and b_i. The large logarithms $(\ln m_W/t)$ coming from QCD radiative corrections to four quark operators are included in the Wilson coefficients $C(t)$. The large double logarithms $(\ln^2 x_i)$ on the longitudinal direction are summed by the threshold resummation [19], and they lead to $S_t(x_i)$ which smears the end-point singularities on x_i. The last term, $e^{-S(t)}$, is the Sudakov form factor resulting from overlap of soft and collinear divergences, which suppresses the soft dynamics effectively [20]. Thus it makes the perturbative calculation of the hard part H applicable at intermediate scale, i.e., M_{B_s} scale. We will calculate analytically the function $H(x_i, b_i, t)$ for $B_s \to \rho(\omega)K$ decays in the first order in α_s expansion and give the convoluted amplitudes in next section.

A. Wilson Coefficients

It is well known that the low-energy effective Hamiltonian is the basic tool to calculate the branching ratios and $\mathcal{A}_{CP}$ of B meson decays. For $B_s \to \rho(\omega)K$ decays, the related weak effective Hamiltonian H_{eff} can be written as [21]

$$\mathcal{H}_{eff} = \frac{G_F}{\sqrt{2}} \left[V_{ub}V_{ud}^* \left(C_1(\mu) O_1^u(\mu) + C_2(\mu) O_2^u(\mu) \right) - V_{tb}V_{td}^* \sum_{i=3}^{10} C_i(\mu)\, O_i(\mu) \right] . \tag{5}$$

We specify below the operators in $\mathcal{H}_{eff}$ for $b \to d$ transition:

$$\begin{array}{llll}
O_1^u &= \bar{d}_\alpha \gamma^\mu L u_\beta \cdot \bar{u}_\beta \gamma_\mu L b_\alpha \ , & O_2^u &= \bar{d}_\alpha \gamma^\mu L u_\alpha \cdot \bar{u}_\beta \gamma_\mu L b_\beta \ , \\
O_3 &= \bar{d}_\alpha \gamma^\mu L b_\alpha \cdot \sum_{q'} \bar{q}'_\beta \gamma_\mu L q'_\beta \ , & O_4 &= \bar{d}_\alpha \gamma^\mu L b_\beta \cdot \sum_{q'} \bar{q}'_\beta \gamma_\mu L q'_\alpha \ , \\
O_5 &= \bar{d}_\alpha \gamma^\mu L b_\alpha \cdot \sum_{q'} \bar{q}'_\beta \gamma_\mu R q'_\beta \ , & O_6 &= \bar{d}_\alpha \gamma^\mu L b_\beta \cdot \sum_{q'} \bar{q}'_\beta \gamma_\mu R q'_\alpha \ , \\
O_7 &= \frac{3}{2} \bar{d}_\alpha \gamma^\mu L b_\alpha \cdot \sum_{q'} e_{q'} \bar{q}'_\beta \gamma_\mu R q'_\beta \ , & O_8 &= \frac{3}{2} \bar{d}_\alpha \gamma^\mu L b_\beta \cdot \sum_{q'} e_{q'} \bar{q}'_\beta \gamma_\mu R q'_\alpha \ , \\
O_9 &= \frac{3}{2} \bar{d}_\alpha \gamma^\mu L b_\alpha \cdot \sum_{q'} e_{q'} \bar{q}'_\beta \gamma_\mu L q'_\beta \ , & O_{10} &= \frac{3}{2} \bar{d}_\alpha \gamma^\mu L b_\beta \cdot \sum_{q'} e_{q'} \bar{q}'_\beta \gamma_\mu L q'_\alpha \ ,
\end{array} \tag{6}$$

where α and β are the $SU(3)$ color indices; L and R are the left- and right-handed projection operators with $L = (1 - \gamma_5)$, $R = (1 + \gamma_5)$. The sum over q' runs over the quark fields that are active at the scale $\mu = O(m_b)$, i.e., $(q' \epsilon \{u, d, s, c, b\})$. The pQCD approach works well for the leading twist approximation and leading double logarithm summation. For the Wilson coefficients $C_i(\mu)$ $(i = 1, \ldots, 10)$, we will also use the leading order (LO) expressions, although the next-to-leading order calculations already exist in the literature [21]. This is the consistent way to cancel the explicit μ dependence in the theoretical formulae.

For the renormalization group evolution of the Wilson coefficients from higher scale to lower scale, we use the formulae as given in Ref. [22] directly. At the high m_W scale, the leading order Wilson coefficients $C_i(M_W)$ are simple and can be found easily in Ref. [21]. In pQCD approach, the scale t may be larger or smaller than the m_b scale. For the case of $m_b < t < m_W$, we evaluate the Wilson coefficients at t scale using leading logarithm running equations, as given in Eq.(C1) of Ref. [22]. For the case of $t < m_b$, we then evaluate the Wilson coefficients at t scale by using $C_i(m_b)$ as input and the formulae given in Appendix D of Ref. [22].

B. Wave Functions

In the resummation procedures, the B_s meson is treated as a heavy-light system. In general, the $B_s$meson light-cone matrix element can be decomposed as[6, 23]

$$\begin{aligned}&\int_0^1 \frac{d^4z}{(2\pi)^4} e^{i\mathbf{k_1}\cdot\mathbf{z}} \langle 0|\bar{b}_\alpha(0) s_\beta(z)|B(p_{B_s})\rangle \\ &= -\frac{i}{\sqrt{2N_c}} \left\{ (\not{p}_{B_s} + M_{B_s})\gamma_5 \left[\phi_{B_s}(\mathbf{k_1}) - \frac{\not{n} - \not{v}}{\sqrt{2}} \bar{\phi}_{B_s}(\mathbf{k_1}) \right] \right\}_{\beta\alpha}, \end{aligned} \tag{7}$$

where $n = (1, 0, \mathbf{0_T})$, and $v = (0, 1, \mathbf{0_T})$ are the unit vectors pointing to the plus and minus directions, respectively. From the above equation, one can see that there are two Lorentz structures in the B_s meson distribution amplitudes. They obey to the following normalization conditions

$$\int \frac{d^4k_1}{(2\pi)^4} \phi_{B_s}(\mathbf{k_1}) = \frac{f_{B_s}}{2\sqrt{2N_c}}, \quad \int \frac{d^4k_1}{(2\pi)^4} \bar{\phi}_{B_s}(\mathbf{k_1}) = 0. \tag{8}$$

In general, one should consider these two Lorentz structures in calculations of B_s meson decays. However, it can be argued that the contribution of $\bar{\phi}_{B_s}$ is numerically small, thus its contribution can be numerically neglected. Using this approximation, we can reduce one input parameter in our calculation. Therefore, we only consider the contribution of Lorentz structure

$$\Phi_{B_s} = \frac{1}{\sqrt{2N_c}} (\not{p}_{B_s} + M_{B_s})\gamma_5 \phi_{B_s}(\mathbf{k_1}). \tag{9}$$

In the next section, we will see that the hard part is always independent of one of the k_1^+ and/or k_1^-, if we make approximations shown in next section. The B_s meson wave function is then the function of variable k_1^- (or k_1^+) and $k_1^\perp$,

$$\phi_{B_s}(k_1^-, k_1^\perp) = \int dk_1^+ \phi(k_1^+, k_1^-, k_1^\perp). \tag{10}$$

The wave function for the pseudoscalar meson K are given as:

$$\Phi_K(P, x, \zeta) \equiv \frac{i}{\sqrt{2N_c}} \gamma_5 \left\{ \not{p}_K \phi_K^A(x) + m_0^K \phi_K^P(x) + \zeta m_0^K (\not{v}\not{n} - v\cdot n) \phi_K^T(x) \right\} \tag{11}$$

where P and x are the momentum and the momentum fraction of K meson, respectively. We assumed here that the wave function of K meson is the same as the wave function of π meson. The parameter ζ is either $+1$ or -1 depending on the assignment of the momentum fraction x.

For $B \to \rho K$ decay, the ρ meson is longitudinally polarized. We only consider its wave function in longitudinal polarization [24, 25],

$$< \rho^-(P, \epsilon_L)|\bar{d}_\alpha(z) u_\beta(0)|0 >= \frac{1}{\sqrt{2N_c}} \int_0^1 dx e^{ixP\cdot z} \left\{ \not{\epsilon} \left[\not{p}_\rho \phi_\rho^t(x) + m_\rho \phi_\rho(x) \right] + m_\rho \phi_\rho^s(x) \right\} \tag{12}$$

The second term in above equation is the leading twist wave function (twist-2), while the first and third terms are sub-leading twist (twist-3) wave functions. For $B \to \omega K$ decay, we have similar expression as Eq. (12).

The transverse momentum $k^\perp$ is usually conveniently converted to the b parameter by Fourier transformation. The initial conditions of function $\phi_i(x)$, $i = B_s, \rho, \omega, k$, are of non-perturbative origin, satisfying the normalization relation

$$\int_0^1 \phi_i(x, b=0)dx = \frac{1}{2\sqrt{6}} f_i \ , \tag{13}$$

with f_i the meson decay constants.

III. PERTURBATIVE CALCULATIONS

In the previous section we have discussed the wave functions and Wilson coefficients of the amplitude in eq.(1). In this section, we will calculate the hard part $H(t)$. This part involves the four quark operators and the necessary hard gluon connecting the four quark operator and the spectator quark. We will show the whole amplitude for each diagram including wave functions. Similar to the $B_s \to \pi K$ [14], the total 8 lowest order diagrams contributing to the $B_s \to \rho K$ decays, are illustrated in Figure 1. We first calculate the usual factorizable diagrams (a) and (b). Operators O_1, O_2, O_3, O_4, O_9, and O_{10} are $(V-A)(V-A)$ currents, the sum of their amplitudes is given as

$$\begin{aligned} F_{eK} \ = \ & -8\pi C_F f_\rho M_{B_s}^4 \int_0^1 dx_1 dx_3 \int_0^\infty b_1 db_1 b_3 db_3 \, \phi_{B_s}(x_1, b_1) \\ & \cdot \Big\{ \big[(2-x_3)\phi_K^A(x_3, b_3) + (2x_3-1) r_K (\phi_K^P(x_3, b_3) - \phi_K^T(x_3, b_3)) \big] \\ & \alpha_s(t_e^1) h_e(x_1, 1-x_3, b_1, b_3) \exp[-S_{ab}(t_e^1)] \\ & + 2 r_k \phi_K^P(x_3, b_3) \alpha_s(t_e^2) h_e(1-x_3, x_1, b_3, b_1) \exp[-S_{ab}(t_e^2)] \Big\} \ , \end{aligned} \tag{14}$$

where $C_F = 4/3$ is a color factor. The function h_e^i, the energy scales t_e^i and the Sudakov factors S_{ab} are displayed in the Appendix. In the above equation, we do not include the Wilson coefficients of the corresponding operators, which are process dependent. They will be shown later in this section for different decay channels. The diagrams Fig. 1(a) and 1(b) are also the diagrams for the $B_s \to K$ form factor $F_0^{B_s \to K}$. Therefore we can extract $F_0^{B_s \to K}$ from Eq. (14).

The operators O_5, O_6, O_7, and O_8 have a structure of $(V-A)(V+A)$. In some decay channels, some of these operators contribute to the decay amplitude in a factorizable way. Since only the axial-vector part of $(V+A)$ current contribute to the pseudo-scaler meson production,

$$\langle \rho | V-A | B \rangle \langle K | V+A | 0 \rangle = - \langle \rho | V-A | B \rangle \langle K | V-A | 0 \rangle, \tag{15}$$

the result of these $(V-A)(V+A)$ operators is opposite to Eq. (14), i.e.,

$$F_{eK}^{P_1} \ = \ -F_{eK}. \tag{16}$$

In some other cases, we need to do Fierz transformation for these operators to get right color structure for factorization to work. In this case, we get $(S+P)(S-P)$ operators

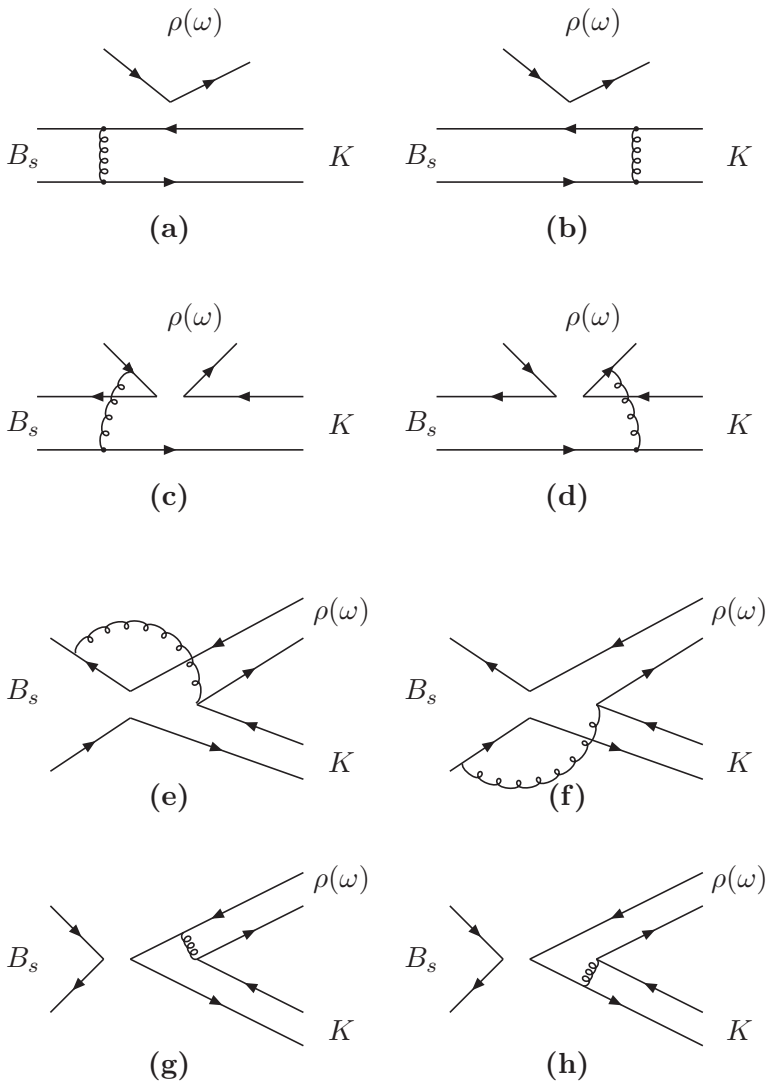

FIG. 1: Diagrams contributing to the $B_s \to \rho K$ and ωK decays (diagram (a) and (b) contribute to the $B_s \to K$ form factor $F_0^{B_s \to K}$).

from $(V-A)(V+A)$ ones. For these $(S+P)(S-P)$ operators, Fig. 1(a) and 1(b) will give

$$F_{eK}^{P_2} \;=\; 0\,. \tag{17}$$

For the non-factorizable diagram 1(c) and 1(d), all three meson wave functions are involved. The integration of b_3 can be performed using δ function $\delta(b_3 - b_1)$, leaving only integration of b_1 and b_2. For the $(V-A)(V-A)$ operators, the result is:

$$\begin{aligned} M_{eK} \;=\; & \frac{32}{\sqrt{6}}\pi C_F M_{B_s}^4 \int_0^1 dx_1 dx_2\, dx_3 \int_0^\infty b_1 db_1 b_2 db_2\, \phi_{B_s}(x_1,b_1)\phi_\rho(x_2,b_2) \\ & \cdot \{(1-x_3)\left[\phi_K^A(x_3,b_1) + 2r_k\phi_K^T(x_3,b_1)\right] \\ & \cdot \alpha_s(t_f) h_f(x_1,x_2,1-x_3,b_1,b_2)\exp[-S_{cd}(t_f)]\}\,. \end{aligned} \tag{18}$$

For the $(V-A)(V+A)$ operators, the result is:

$$\begin{aligned} M_{eK}^{P_1} &= \frac{64}{\sqrt{6}}\pi C_F G_F M_{B_s}^4 r_\rho \int_0^1 dx_1 dx_2\, dx_3 \int_0^\infty b_1 db_1 b_2 db_2\, \phi_{B_s}(x_1,b_1) \\ &\cdot \Big\{ \Big[x_2 \phi_K^A(x_3,b_1) \left(\phi_\rho^s(x_2,b_2) - \phi_\rho^t(x_2,b_2)\right) + r_K \left((1+x_2-x_3)\right. \\ &\left(\phi_K^P(x_3,b_1)\phi_\rho^s(x_2,b_2) - \phi_K^T(x_3,b_1)\phi_\rho^t(x_2,b_2)\right) + (1-x_2-x_3) \\ &\left.\left(\phi_K^P(x_3,b_1)\phi_\rho^t(x_2,b_2) - \phi_K^T(x_3,b_1)\phi_\rho^s(x_2,b_2)\right)\right)\Big] \\ &\alpha_s(t_f) h_f(x_1,x_2,1-x_3,b_1,b_2) \exp[-S_{cd}(t_f)] \Big\}\ . \end{aligned} \tag{19}$$

For the $(S-P)(S+P)$ operators, the result is:

$$M_{eK}^{P_2} = -M_{eK}\ . \tag{20}$$

For the non-factorizable annihilation diagram 1(e) and 1(f), again all three wave functions are involved. Here we have two kinds of contributions. M_{ak} is the contribution containing operator type $(V-A)(V-A)$, while $M_{aK}^{P_1}$ is the contribution containing operator type $(V-A)(V+A)$:

$$\begin{aligned} M_{aK} &= \frac{32}{\sqrt{6}}\pi C_F M_{B_s}^4 \int_0^1 dx_1 dx_2\, dx_3 \int_0^\infty b_1 db_1 b_2 db_2\, \phi_{B_s}(x_1,b_1) \\ &\cdot \Big\{ \Big[x_2 \phi_\rho(x_2,b_2) \phi_K^A(x_3,b_2) + r_\rho r_K \left((x_2-x_3)\right. \\ &\cdot \left(\phi_K^P(x_3,b_2)\phi_\rho^t(x_2,b_2) + \phi_K^T(x_3,b_2)\phi_\rho^s(x_2,b_2)\right) + (2+x2+x3) \\ &\cdot \left.\phi_K^P(x_3,b_2)\phi_\rho^s(x_2,b_2) + (-2+x_2+x_3)\phi_K^T(x_3,b_2)\phi_\rho^t(x_2,b_2)\right)\Big] \\ &\cdot \alpha_s(t_f^2) h_f^2(x_1,x_2,x_3,b_1,b_2) \exp[-S_{ef}(t_f^2)] \\ &+ \Big[-x_3 \phi_\rho(x_2,b_2)\phi_K^A(x_3,b_2) + r_\rho r_K \left((x_2-x_3)\left(\phi_K^P(x_3,b_2)\phi_\rho^t(x_2,b_2) + \phi_K^T(x_3,b_2)\right.\right. \\ &\cdot \left.\left.\phi_\rho^s(x_2,b_2)\right) - (x_2+x_3)\left(\phi_K^P(x_3,b_2)\phi_\rho^s(x_2,b_2) + \phi_K^T(x_3,b_2)\phi_\rho^t(x_2,b_2)\right)\right)\Big] \\ &\cdot \alpha_s(t_f^1) h_f^1(x_1,x_2,x_3,b_1,b_2) \exp[-S_{ef}(t_f^1)] \Big\}\ , \end{aligned} \tag{21}$$

$$\begin{aligned} M_{aK}^{P_1} &= \frac{32}{\sqrt{6}}\pi C_F M_{B_s}^4 \int_0^1 dx_1 dx_2\, dx_3 \int_0^\infty b_1 db_1 b_2 db_2\, \phi_{B_s}(x_1,b_1) \\ &\cdot \Big\{ \Big[r_\rho (x_2-2) \phi_K^A(x_3,b_2) \left(\phi_\rho^t(x_2,b_2) + \phi_\rho^s(x_2,b_2)\right) \\ &+ r_K (2-x_3) \phi_\rho(x_2,b_2) \left(\phi_K^P(x_3,b_2) + \phi_K^T(x_3,b_2)\right)\Big] \\ &\cdot \alpha_s(t_f^2) h_f^2(x_1,x_2,x_3,b_1,b_2) \exp[-S_{ef}(t_f^2)] \\ &+ \Big[r_\rho (-x_2) \phi_K^A(x_3,b_2) \left(\phi_\rho^t(x_2,b_2) + \phi_\rho^s(x_2,b_2)\right) \\ &+ r_K x_3 \phi_\rho(x_2,b_2) \left(\phi_K^P(x_3,b_2) + \phi_K^T(x_3,b_2)\right)\Big] \\ &\cdot \alpha_s(t_f^1) h_f^1(x_1,x_2,x_3,b_1,b_2) \exp[-S_{ef}(t_f^1)] \Big\}\ , \end{aligned} \tag{22}$$

where $r_K = m_0^K/M_{B_s}$ and $r_\rho = m_\rho/M_{B_s}$.

The factorizable annihilation diagram 1(g) and 1(h) involve only ρ and K wave functions. There are also two kinds of decay amplitudes for these two diagrams. F_{aK} is for

$(V-A)(V-A)$ type operators, and $F_{aK}^{P_2}$ is for $(S-P)(S+P)$ type operators,

$$\begin{aligned} F_{aK} &= 8\pi C_F f_{B_s} M_{B_s}^4 \int_0^1 dx_2\, dx_3 \int_0^\infty b_2 db_2 b_3 db_3 \\ &\cdot \Big\{ \Big[x_3 \phi_\rho(x_2,b_2) \phi_K^A(x_3,b_3) + 2 r_\rho r_k \phi_\rho^s(x_2,b_2) \Big((1+x_3)\phi_K^P(x_3,b_3) \\ &(x_3-1)\phi_K^T(x_3,b_3) \Big) \Big] \alpha_s(t_e^3) h_a(x_2,x_3,b_2,b_3) \exp[-S_{gh}(t_e^3)] \\ &- \Big[x_2 \phi_\rho(x_2,b_2) \phi_K^A(x_3,b_3) + 2 r_\rho r_k \phi_K^P(x_3,b_3) \Big((1+x_2)\phi_\rho^s(x_2,b_2) \\ &(x_2-1)\phi_\rho^t(x_2,b_2) \Big) \Big] \alpha_s(t_e^4) h_a(x_3,x_2,b_3,b_2) \exp[-S_{gh}(t_e^4)] \Big\} \ , \end{aligned} \tag{23}$$

$$\begin{aligned} F_{aK}^{P_2} &= -16\pi C_F f_{B_s} M_{B_s}^4 \int_0^1 dx_2\, dx_3 \int_0^\infty b_2 db_2 b_3 db_3 \\ &\cdot \Big\{ \Big[2 r_\rho \phi_\rho^s(x_2,b_2) \phi_K^A(x_3,b_3) + r_k x_3 \phi_\rho(x_2,b_2) \Big(\phi_K^P(x_3,b_3) \\ &-\phi_K^T(x_3,b_3) \Big) \Big] \alpha_s(t_e^3) h_a(x_2,x_3,b_2,b_3) \exp[-S_{gh}(t_e^3)] \\ &+ \Big[x_2 r_\rho \phi_K^A(x_3,b_3) \Big(\phi_\rho^s(x_2,b_2) - \phi_\rho^t(x_2,b_2) \Big) + 2 r_k \phi_\rho(x_2,b_2) \\ &\cdot \phi_K^P(x_3,b_3) \alpha_s(t_e^4) h_a(x_3,x_2,b_3,b_2) \exp[-S_{gh}(t_e^4)] \Big\} \ . \end{aligned} \tag{24}$$

In the above equations, we have assumed that $x_1 << x_2, x_3$. Since the light quark momentum fraction x_1 in B meson is peaked at the small x_1 region, this is not a bad approximation. The numerical results also show that this approximation makes very little difference in the final result. After using this approximation, all the diagrams are functions of $k_1^- = x_1 M_{B_s}/\sqrt{2}$ of B_s meson only, independent of the variable of k_1^+. Therefore the integration of eq.(10) is performed safely.

Combining the contributions from different diagrams, the total decay amplitude for $B_s \to \rho^+ K^-$ decay can be written as:

$$\begin{aligned} \mathcal{M}(\rho^+ K^-) &= F_{eK} \left[\xi_u \left(\frac{1}{3} C_1 + C_2 \right) - \xi_t \left(\frac{1}{3} C_3 + C_4 + \frac{1}{3} C_9 + C_{10} \right) \right] \\ &+ M_{eK} \left[\xi_u \left(C_1 \right) - \xi_t \left(C_3 + C_9 \right) \right] + M_{eK}^{P_1} \left[-\xi_t \left(C_5 + C_7 \right) \right] \\ &+ M_{aK} \left[-\xi_t \left(C_3 - \frac{1}{2} C_9 \right) \right] + M_{aK}^{P_1} \left[-\xi_t \left(C_5 - \frac{1}{2} C_7 \right) \right] \\ &+ F_{aK} \left[-\xi_t \left(\frac{1}{3} C_3 + C_4 - \frac{1}{6} C_9 - \frac{1}{2} C_{10} \right) \right] \\ &+ F_{aK}^{P_2} \left[-\xi_t \left(\frac{1}{3} C_5 + C_6 - \frac{1}{6} C_7 - \frac{1}{2} C_8 \right) \right], \end{aligned} \tag{25}$$

where $\xi_u = V_{ub}^* V_{ud}$, $\xi_t = V_{tb}^* V_{td}$

Similarly, the decay amplitude for $B_s \to \rho^0 \overline{K}^0$ can be written as:

$$\begin{aligned}
\mathcal{M}(\rho^0\overline{K}^0) \;=\; & F_{eK}\left[\xi_u\left(C_1+\frac{1}{3}C_2\right)-\xi_t\left(-\frac{1}{3}C_3-C_4+\frac{3}{2}C_7+\frac{1}{2}C_8+\frac{5}{3}C_9+C_{10}\right)\right]f_1 \\
& +M_{eK}\left[\xi_u C_2-\xi_t\left(-C_3-\frac{3}{2}C_8+\frac{1}{2}C_9+\frac{3}{2}C_{10}\right)\right]f_1 \\
& +M_{eK}^{P_1}\left[-\xi_t\left(-C_5+\frac{1}{2}C_7\right)\right]f_1+M_{aK}\left[-\xi_t\left(-C_3+\frac{1}{2}C_9\right)\right]f_1 \\
& +M_{aK}^{P_1}\left[-\xi_t\left(-C_5+\frac{1}{2}C_7\right)\right]f_1+F_{aK}\left[-\xi_t\left(-\frac{1}{3}C_3-C_4+\frac{1}{6}C_9+\frac{1}{2}C_{10}\right)\right]f_1 \\
& +F_{aK}^{P_2}\left[-\xi_t\left(-\frac{1}{3}C_5-C_6+\frac{1}{6}C_7+\frac{1}{2}C_8\right)\right]f_1, \qquad (26)
\end{aligned}$$

where $f_1 = 1/\sqrt{2}$.

For the decay amplitude of $B_s \to \omega\overline{K}^0$ decay, one can obtain its decay amplitude from Eq. (26) by replacing the vector meson ρ with ω, i.e,

$$f_\rho \to f_\omega, \quad f_\rho^T \to f_\omega^T, \quad m_\rho \to m_\omega. \qquad (27)$$

Note that we have considered the difference in the quark components for the two scalar mesons K^+ and K^0 in the analytic expressions. We denote the corresponding amplitudes for $B_s \to \omega\overline{K}^0$ decay as F'_{eK}, M'_{eK}, $M'^{P_1}_{eK}$, M'_{aK}, $M'^{P_1}_{aK}$, F'_{aK} and $F'^{P_2}_{aK}$, but do not show explicit expressions of these amplitudes here for the sake of simplicity. The total amplitude finally can be written as

$$\begin{aligned}
\mathcal{M}(\omega\overline{K}^0) \;=\; & F'_{eK}\left[\xi_u\left(C_1+\frac{1}{3}C_2\right)f_1-\xi_t\left(\frac{7}{3}C_3+\frac{5}{3}C_4\right.\right. \\
& \left.\left.+2C_5+\frac{2}{3}C_6+\frac{1}{2}C_7+\frac{1}{6}C_8+\frac{1}{3}C_9-\frac{1}{3}C_{10}\right)f_1\right] \\
& +M'_{eK}\left[\xi_u\left(C_2\right)f_1-\xi_t\left(C_3+2C_4-2C_6-\frac{1}{2}C_8-\frac{1}{2}C_9+\frac{1}{2}C_{10}\right)f_1\right] \\
& -M'^{P_1}_{eK}\,\xi_t\left(C_5-\frac{1}{2}C_7\right)f_1-M'_{aK}\,\xi_t\left(C_3-\frac{1}{2}C_9\right)f_1 \\
& -M'^{P_1}_{aK}\,\xi_t\left(C_5-\frac{1}{2}C_7\right)f_1-F'_{aK}\,\xi_t\left(\frac{1}{3}C_3+C_4-\frac{1}{6}C_9-\frac{1}{2}C_{10}\right)f_1 \\
& +F'^{P_2}_{aK}\,\xi_t\left(\frac{1}{3}C_5+C_6-\frac{1}{6}C_7-\frac{1}{2}C_8\right)f_1, \qquad (28)
\end{aligned}$$

where $f_1 = 1/\sqrt{2}$.

IV. NUMERICAL RESULTS AND DISCUSSIONS

A. Input parameters and wave functions

In the numerical calculations we use the following input parameters

$$\begin{aligned}
\Lambda_{\overline{\rm MS}}^{(f=4)} &= 250{\rm MeV}, \quad f_\rho = 205{\rm MeV}, \quad f_\rho^T = 160{\rm MeV}, \\
m_0^K &= 1.6{\rm GeV}, \quad f_{B_s} = 236{\rm MeV}, \quad f_K = 160{\rm MeV}, \\
m_\omega &= 0.782{\rm GeV}, \quad f_\omega = 200{\rm MeV}, \quad f_\omega^T = 160{\rm MeV}, \\
m_\rho &= 0.770{\rm GeV}, \quad M_{B_s} = 5.37{\rm GeV}, \quad M_W = 80.42{\rm GeV}.
\end{aligned} \tag{29}$$

The central values of the CKM matrix elements to be used in numerical calculations are [26]

$$|V_{ud}| = 0.9745, \quad |V_{ub}| = 0.0038, \quad |V_{tb}| = 1, \quad |V_{td}| = 0.0083. \tag{30}$$

For the B_s meson wave function, we adopt the model

$$\phi_{B_s}(x,b) = N_{B_s} x^2(1-x)^2 \exp\left[-\frac{M_{B_s}^2\, x^2}{2\omega_b^2} - \frac{1}{2}(\omega_b b)^2\right], \tag{31}$$

where ω_b is a free parameter and we take $\omega_b = 0.5 \pm 0.05$ GeV in numerical calculations, and $N_{B_s} = 65.332$ is the normalization factor for $\omega_b = 0.5$. This is the same wave function as used in Refs. [9, 12, 27].

For the light meson wave function, we neglect the b dependant part, which is not important in numerical analysis. We choose the wave function of ρ and ω meson as given in Ref. [25]

$$\phi_{\rho(\omega)}(x) = \frac{3}{\sqrt{6}} f_{\rho(\omega)} x(1-x)\left[1 + 0.18 C_2^{3/2}(2x-1)\right], \tag{32}$$

$$\begin{aligned}
\phi_{\rho(\omega)}^t(x) &= \frac{f_{\rho(\omega)}^T}{2\sqrt{6}}\left\{3(2x-1)^2 + 0.3(2x-1)^2\left[5(2x-1)^2 - 3\right]\right. \\
&\quad \left. + 0.21[3 - 30(2x-1)^2 + 35(2x-1)^4]\right\},
\end{aligned} \tag{33}$$

$$\phi_{\rho(\omega)}^s(x) = \frac{3}{2\sqrt{6}} f_{\rho(\omega)}^T (1-2x)\left[1 + 0.76(10x^2 - 10x + 1)\right]. \tag{34}$$

The Gegenbauer polynomial is defined by

$$C_2^{3/2}(t) = \frac{3}{2}\left(5t^2 - 1\right). \tag{35}$$

For K meson's wave functions, ϕ_K^A, ϕ_K^P and ϕ_K^T describe the axial vector, pseudoscalar and tensor components respectively. We utilize the result from the light-cone sum rule [28] including twist-3 contribution:

$$\begin{aligned}
\phi_K^A(x) &= \frac{3}{\sqrt{2N_c}} f_K x(1-x)\left[1 + 0.15t + 0.405\left(5t^2 - 1\right)\right], \\
\phi_K^P(x) &= \frac{1}{2\sqrt{2N_c}} f_K \left[1 + 0.106\left(3t^2 - 1\right) - \frac{0.148}{8}\left(3 - 30t^2 + 35t^4\right)\right], \\
\phi_K^T(x) &= \frac{1}{2\sqrt{2N_c}} f_K\, t\left[1 + 0.1581\left(5t^2 - 3\right)\right].
\end{aligned} \tag{36}$$

whose coefficients correspond to $m_0^K = 1.6$ GeV and $t = 1 - 2x$. The parameter m_0^K is defined as:

$$m_0^K \equiv \frac{m_K^2}{(m_u + m_s)} \, . \tag{37}$$

For the pseudoscalar K meson we have assumed that the wave function of $\overline{K^0}$ is the same as the wave function of K^-, since one can assume that the mass of the u quark is equivalent to the mass of the d quark due to the isospin symmetry.

We include full expression of twist-3 wave functions for light mesons. The twist-3 wave functions are also adopted from QCD sum rule calculations [29]. Using the above chosen wave functions and the relevant input parameters, we find the numerical value of the corresponding form factor at zero momentum transfer from Eqs.(14):

$$F_0^{B_s \to K}(q^2 = 0) \; = \; \frac{F_{eK}}{m_{B_s}^2} = 0.276^{+0.050}_{-0.040} \, , \tag{38}$$

for $\omega_b = 0.50 \pm 0.05$ GeV, which agrees well with the value as given in Refs. [14, 30].

B. Branching ratios

For $B_s \to \rho(\omega) K$ decays, the decay amplitudes as given in Eqs. (25), (26) and (28) can be rewritten as

$$\mathcal{M} \; = \; V_{ub}^* V_{ud} T - V_{tb}^* V_{td} P = V_{ub}^* V_{ud} T \left[1 + z e^{i(\alpha + \delta)} \right] , \tag{39}$$

where $\alpha = \arg \left[-\frac{V_{td} V_{tb}^*}{V_{ud} V_{ub}^*} \right]$ is the weak phase (one of the three CKM angles), and δ is the relative strong phase between the tree ("T") and penguin ("P") amplitude, while the term "z" describes the ratio of penguin to tree contributions and is defined as

$$z = \left| \frac{V_{tb}^* V_{td}}{V_{ub}^* V_{ud}} \right| \left| \frac{P}{T} \right| . \tag{40}$$

The ratio z and the strong phase δ can be calculated in the pQCD approach. For $B_s \to \rho^+ K^-$, $\rho^0 \overline{K}^0$ and $\omega \overline{K}^0$ decays, we find numerically that

$$z(\rho^+ K^-) \; = \; 0.10, \quad \delta(\rho^+ K^-) = +138^\circ, \tag{41}$$

$$z(\rho^0 \overline{K}^0) \; = \; 1.5, \quad \delta(\rho^0 \overline{K}^0) = +77^\circ, \tag{42}$$

$$z(\omega \overline{K}^0) \; = \; 1.9, \quad \delta(\omega \overline{K}^0) = +273^\circ. \tag{43}$$

For $B_s \to \rho \overline{K}^0$ and $B_s \to \omega \overline{K}^0$ decays, the "Tree" diagram contribution is suppressed by a factor of $C_1 + C_2/3 \sim 0.1$. Thus the penguin diagram contribution is comparable with the tree contribution. In our calculation, the only input parameters are wave functions,which stand for the non-perturbative contributions. Up to now, no exact solution is made for them. So the main uncertainty in pQCD approach comes from these wave functions. In this paper, we choose the light cone wave functions which are obtained from QCD Sum

Rules [28, 29]. For heavy B and B_s mesons, its wave function is still under discussion using different approaches. In this paper, we find the branching ratio of $B_s \to \rho(\omega)K$ is sensitive to the wave function parameter ω_b. So the main errors of the ratio z and the strong phase δ are induced by the uncertainty of $\omega_b = 0.5 \pm 0.05$ GeV. We just use the central values of z and δ in the following numerical calculations, unless stated explicitly.

From Eq. (39), it is easy to write the decay amplitude $\overline{\mathcal{M}}$ for the corresponding charge conjugated decay mode. And the CP-averaged branching ratio for considered decays is generally defined as

$$Br = (|\mathcal{M}|^2 + |\overline{\mathcal{M}}|^2)/2 = |V_{ub}V_{ud}^* T|^2 \left[1 + 2z\cos\alpha\cos\delta + z^2\right], \tag{44}$$

where the ratio z and the strong phase δ have been defined in Eqs.(39) and (40).

Using the wave functions and the input parameters as specified in previous sections, it is straightforward to calculate the CP averaged branching ratios for the three considered decays. The theoretical predictions in the pQCD approach for the branching ratios of the decays under consideration are the following:

$$Br(B_s \to \rho^\pm K^\mp) = \left[24.7^{+10.1}_{-6.7}(\omega_b)^{+1.1}_{-1.2}(\alpha)\right] \times 10^{-6}, \tag{45}$$

$$Br(B_s \to \rho^0 \overline{K}^0) = \left[1.2^{+0.4}_{-0.2}(\omega_b) \pm 0.1(\alpha)\right] \times 10^{-7}, \tag{46}$$

$$Br(B_s \to \omega \overline{K}^0) = \left[1.7^{+0.6}_{-0.3}(\omega_b) \pm 0.02(\alpha)\right] \times 10^{-7}, \tag{47}$$

where the major errors are induced by the uncertainty of $\omega_b = 0.5 \pm 0.05$ GeV, and $\alpha = 100^\circ \pm 20^\circ$, respectively. It is easy to see that the above pQCD predictions for the branching ratios are consistent with those predicted in the QCD factorization approach [10],

$$Br(B_s \to \rho^\pm K^\mp) = \left[24.5^{+15.2}_{-12.9}\right] \times 10^{-6}, \tag{48}$$

$$Br(B_s \to \rho^0 \overline{K}^0) = \left[6.1^{+12.6}_{-6.0}\right] \times 10^{-7}, \tag{49}$$

$$Br(B_s \to \omega \overline{K}^0) = \left[5.1^{+8.3}_{-4.0}\right] \times 10^{-7}, \tag{50}$$

within one standard deviation, although the central values of pQCD predictions for $B_s \to (\rho^0, \omega)\overline{K}^0$ decays are much smaller than those in QCD factorization approach.

In Figs. 2 and 3, we show the α-dependence of the pQCD predictions for the CP averaged branching ratios of $B_s \to \rho^\pm K^\mp$, $\rho^0\overline{K}^0$ and $\omega\overline{K}^0$ decays for $\alpha = [0^\circ, 180^\circ]$ and $\omega_b = 0.5 \pm 0.05$ GeV.

It is worth stressing that the theoretical predictions in the pQCD approach have large theoretical errors induced by the large uncertainties of parameter ω_b and CKM angle α. From Figs. 2 and 3, we observe that the pQCD predictions are sensitive to the variations of ω_b. This sensitive dependence could be fixed by the well measured $B_s \to K$ form factors from the semi-leptonic B_s decays as expected in LHCb experiment. Other uncertainties in our calculation include the next-to-leading order α_s QCD corrections and higher twist contributions, which need more complicated calculations. The parameter $m_0^K \approx 1.6$ GeV characterizes the relative size of twist 3 contribution to twist 2 contribution. Because of the chiral enhancement of m_0^K, the twist 3 contribution become comparable in size with the twist 2 contribution.

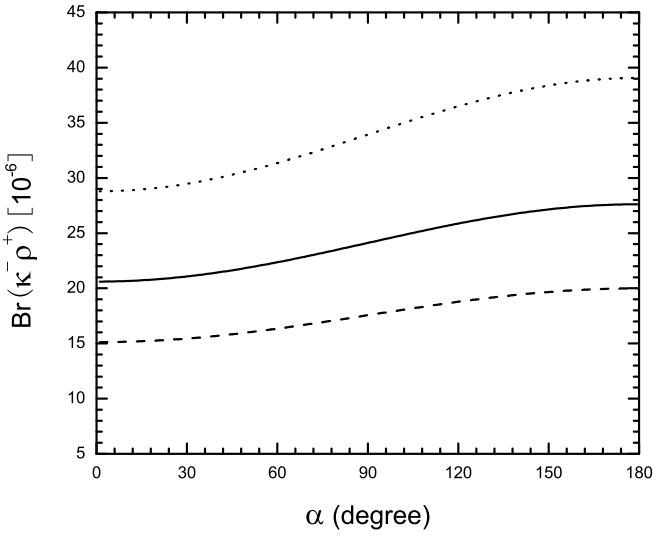

FIG. 2: The branching ratio (in unit of 10^{-6}) of $B_s \to \rho^{\pm} K^{\mp}$ decay for $\omega_b = 0.45$ GeV (dotted curve), 0.50 GeV (solid curve) and 0.55 GeV (dashed curve), as a function of the CKM angle α.

C. CP-violating asymmetries

Now we turn to the evaluations of the CP-violating asymmetries of $B_s \to \rho(\omega)K$ decays in pQCD approach. For $B_s \to \rho^+ K^-$ decay, the direct CP-violating asymmetry $\mathcal{A}_{CP}$ can be defined as:

$$\mathcal{A}_{CP}^{dir} = \frac{|\mathcal{M}|^2 - |\overline{\mathcal{M}}|^2}{|\mathcal{M}|^2 + |\overline{\mathcal{M}}|^2} = \frac{-2z \sin\alpha \sin\delta}{1 + 2z\cos\alpha\cos\delta + z^2}, \tag{51}$$

where the ratio z and the strong phase δ have been defined in previous subsection and are calculable in pQCD approach.

Using the central values of z and δ as given in Eqs.(41) , (42) and (43), it is easy to calculate the CP-violating asymmetries:

$$\mathcal{A}_{CP}^{dir}(B_s \to \rho^{\pm} K^{\mp}) \;=\; (-12.5^{+2.0}_{-2.2}(\omega_b)^{-0.6}_{+2.0}(\alpha)) \times 10^{-2}. \tag{52}$$

Here two major errors are induced by $\omega_b = 0.50 \pm 0.05$ GeV and $\alpha = 100^\circ \pm 20^\circ$. The pQCD prediction in Eq. (52) is also consistent with the prediction in QCDF approach [10] within one standard deviation: $\mathcal{A}_{CP}^{dir}(B_s \to \rho^{\pm} K^{\mp}) = (-1.5 \pm 12.2) \times 10^{-2}$.

In Fig. 4, we show the $\alpha-$dependence of the direct CP-violating asymmetries $\mathcal{A}_{CP}^{dir}$ for $B_s \to \rho^{\pm} K^{\mp}$ decay. The possible theoretical errors induced by the uncertainties of other input parameters are usually not large, since both z and δ are stable against the variations of them. Uncertainties not included here are the next-to-leading order contributions, which may affect the CP asymmetry strongly [31]. For $B_s \to \rho^{\pm} K^{\mp}$ decay, a large CP asymmetry at 10% level plus large branching ratios at 10^{-5} level are clearly measurable in the forthcoming LHCb experiments.

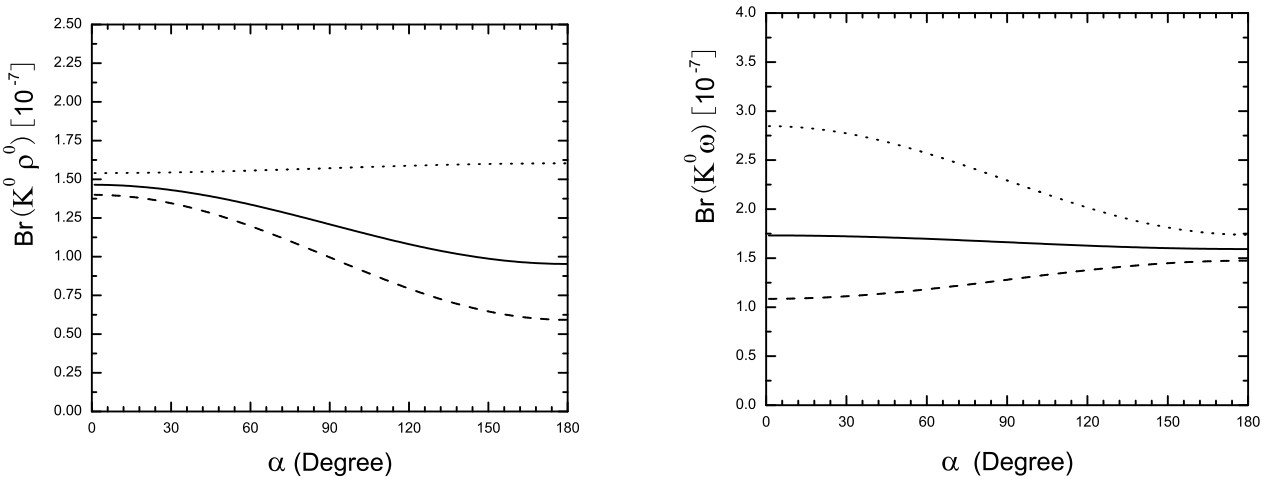

FIG. 3: The branching ratio (in unit of 10^{-7}) of $B_s \to \rho^0 \overline{K}^0$ and $\omega \overline{K}^0$ decays for $\omega_b = 0.45$ GeV (dotted curve), 0.50 GeV(solid curve) and 0.55 GeV(dashed curve), as a function of the CKM angle α.

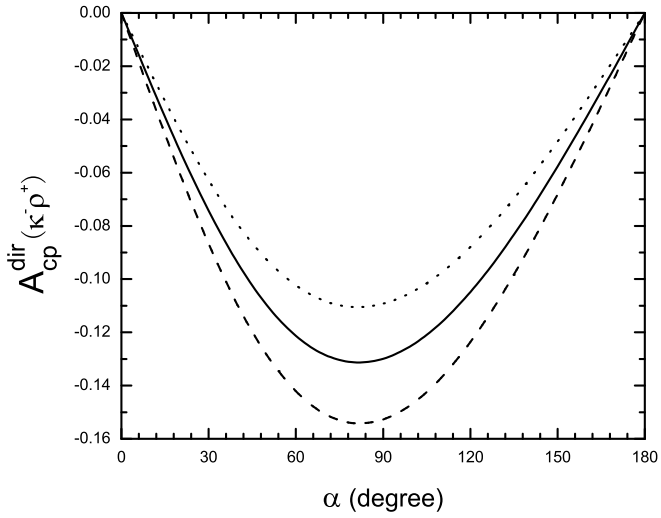

FIG. 4: The α-dependence of the direct CP asymmetries of $B_s \to \rho^{\pm} K^{\mp}$ decay for $\omega_b = 0.45$ GeV (dotted curve), 0.50 GeV (solid curve) and 0.55 GeV (dashed curve).

For the pure neutral decays $B_s \to \rho^0 \overline{K}^0$ and $\omega \overline{K}^0$, there are both direct and mixing-induced CP violation. Using Eq. (51), we find that

$$\begin{aligned} \mathcal{A}_{CP}^{dir}(B_s \to \rho^0 \overline{K}^0) &= (-91.9^{-1.8}_{+8.0}(\omega_b)^{+6.5}_{+4.8}(\alpha)) \times 10^{-2}, \\ \mathcal{A}_{CP}^{dir}(B_s \to \omega \overline{K}^0) &= (+81.2^{+1.7}_{-5.6}(\omega_b)^{-1.2}_{-8.8}(\alpha)) \times 10^{-2}, \end{aligned} \tag{53}$$

for $\omega_b = 0.50 \pm 0.05$ GeV and $\alpha = 100^\circ \pm 20^\circ$. In Fig. 5, we show the $\alpha-$dependence of the direct CP-violating asymmetry for $B_s \to \rho^0 \overline{K}^0$ and $B_s \to \omega \overline{K}^0$ decays.

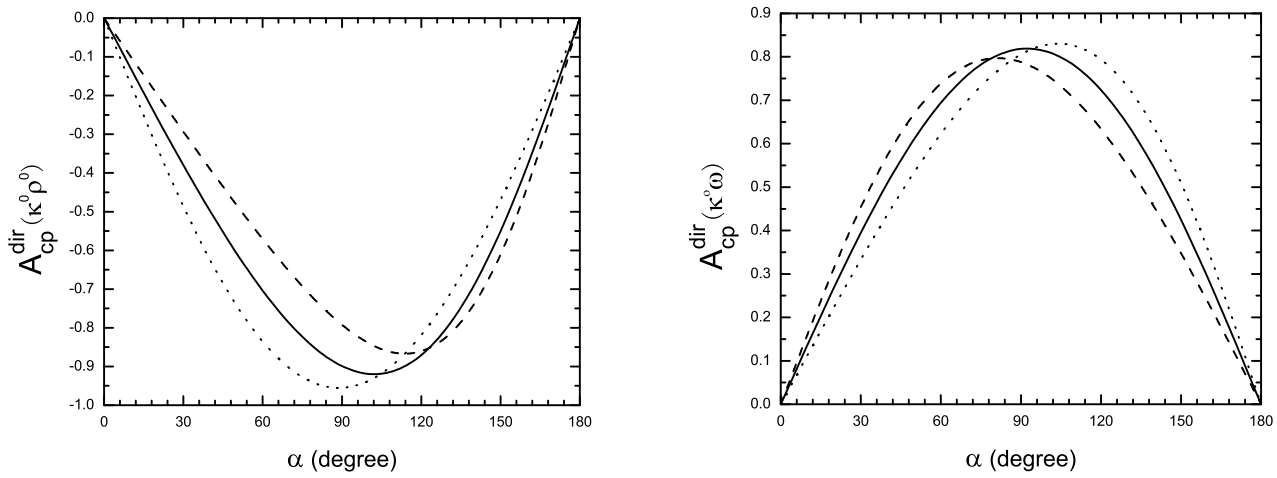

FIG. 5: The α-dependence of the direct CP asymmetries of $B_s \to \rho^0\overline{K}^0$ and $\omega\overline{K}^0$) decays for $\omega_b = 0.45$ GeV (dotted curve), 0.50 GeV (solid curve) and 0.55 GeV (dashed curve).

The pQCD predictions as given in Eq. (53) are quite different from those obtained by using the QCDF approach as given in Refs.[10] :

$$\begin{aligned} \mathcal{A}_{CP}^{dir}(B_s \to \rho^0\overline{K}^0) &= (24.7^{+58.3}_{-56.8}) \times 10^{-2}, \\ \mathcal{A}_{CP}^{dir}(B_s \to \omega\overline{K}^0) &= (-43.9^{+69.1}_{-62.1}) \times 10^{-2}. \end{aligned} \tag{54}$$

The reason is the great difference in the source of strong phases in two facterization approaches. In QCDF approach, the strong phase mainly comes from the perturbative charm quark loop diagram, which is α_s suppressed [10]. But the strong phase in pQCD approach comes mainly from non-factorizable and annihilation type diagrams (see figures 1(c) $\sim$1 (h)). The sign of the direct CP asymmetry is also different for these two approaches for the latter two neutral decays. The forthcoming LHC-b experiments can make a test for these two methods.

Following Ref.[14], the mixing-induced CP asymmetry for $B_s \to \rho^0\overline{K}^0$ and $\omega\overline{K}^0$ decays, can be defined as

$$\mathcal{A}_{CP}^{mix} = \frac{-2Im(\lambda_{CP})}{1+|\lambda_{CP}|^2} = \frac{\sin 2\gamma + 2Re(x)\sin\gamma}{1+|x|^2+2Re(x)\cos\gamma}, \tag{55}$$

where $x = \frac{V_{cb}V_{cd}^*}{|V_{ub}V_{ud}^*|}\frac{P}{T+P}$, and the angle γ is one of the three CKM angles. Numerically, the pQCD predictions for the mixing induced CP asymmetry are

$$\begin{aligned} \mathcal{A}_{CP}^{mix}(B_s \to \rho^0\overline{K}^0) &= (-37^{+22}_{-19}(\omega_b)^{+26}_{+22}(\gamma)) \times 10^{-2}, \\ \mathcal{A}_{CP}^{mix}(B_s \to \omega\overline{K}^0) &= (-40 \pm 11(\omega_b)^{+19}_{-15}(\gamma)) \times 10^{-2}, \end{aligned} \tag{56}$$

for $\omega_b = 0.50 \pm 0.05$ GeV and $\gamma = 60^\circ \pm 20^\circ$. The γ-dependence of the mixing-induced CP asymmetries are shown in Fig. 6

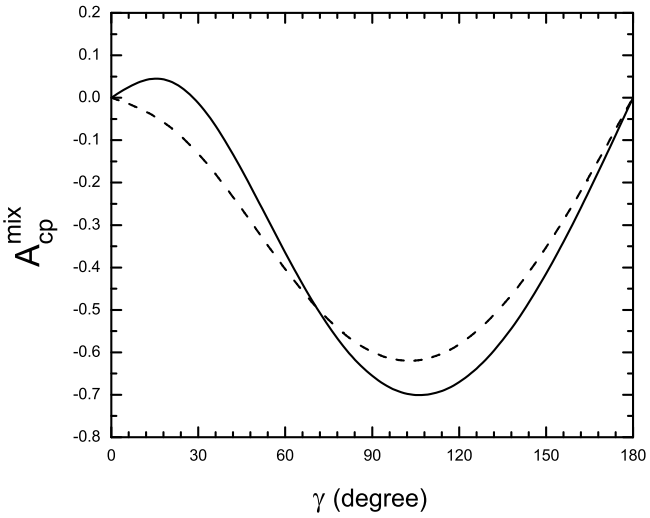

FIG. 6: The γ-dependence of the mixing-induced CP violating asymmetry of $B_s \to \rho^0 \overline{K}^0$ (solid curve) and $B_s \to \omega \overline{K}^0$ (dashed curve) for fixed $\omega_b = 0.50$ GeV.

V. SUMMARY

In this paper, we calculate the branching ratios and CP-violating asymmetries of $B_s \to \rho^{\pm} K^{\mp}$, $\rho^0 \overline{K}^0$ and $\omega \overline{K}^0$ decays in the pQCD factorization approach.

Besides the usual factorizable diagrams, the non-factorizable and annihilation diagrams as shown in Fig. 1 are also calculated analytically. The non-factorizable and annihilation contributions provide the necessary strong phase required by a non-zero CP-violating asymmetry for the considered decays.

From our calculations and phenomenological analysis, we found the following results:

- From analytical calculations, the form factor $F^{B_s \to K}(0)$ can be extracted. The pQCD prediction is $F^{B_s \to K}(0) = 0.276^{+0.050}_{-0.040}$ for $\omega_b = 0.50 \pm 0.05$ GeV, which agrees well with the value as given in Ref. [14] and the result obtained from the QCD sum rule calculations [30].

- For the CP-averaged branching ratios of the three considered decay modes, the pQCD predictions are

$$\begin{aligned} Br(B_s \to \rho^{\pm} K^{\mp}) &\approx 24.7 \times 10^{-6}, \\ Br(B_s \to \rho^0 \overline{K}^0) &\approx 1.2 \times 10^{-7}, \\ Br(B_s \to \omega \overline{K}^0) &\approx 1.7 \times 10^{-7}. \end{aligned} \tag{57}$$

  The theoretical uncertainties are around thirty to fifty percent. The leading pQCD predictions for the branching ratios are also consistent with those obtained by employing the QCD factorization approach.

- For the CP-violating asymmetries, the theoretical predictions in pQCD approach

are

$$\begin{aligned}
\mathcal{A}_{CP}^{dir}(B_s \to \rho^{\pm} K^{\mp}) &\approx -12\%, \\
\mathcal{A}_{CP}^{dir}(B_s \to \rho^0 \overline{K}^0) &\approx -92\%, \quad \mathcal{A}_{CP}^{mix}(B_s \to \rho^0 \overline{K}^0) \approx -36\%, \\
\mathcal{A}_{CP}^{dir}(B_s \to \omega \overline{K}^0) &\approx +81\%, \quad \mathcal{A}_{CP}^{mix}(B_s \to \omega \overline{K}^0) \approx -40\%,
\end{aligned} \tag{58}$$

for $\alpha \approx 100^\circ$, $\gamma \approx 60^\circ$. Of course, the theoretical errors here are still large.

Acknowledgments

We are very grateful to Cai-Dian Lü, Libo Guo, Hui-sheng Wang, Xin Liu and Qian-gui Xu for helpful discussions. This work is partly supported by the National Natural Science Foundation of China under Grant No.10275035 and 10575052, and by the Specialized Research Fund for the Doctoral Program of Higher Education (SRFDP) under Grant No. 20050319008.

APPENDIX A: RELATED FUNCTIONS

We show here the function h_i's appeared in the expressions of the decay amplitudes in Sec. III, coming from the Fourier transformations of function $H^{(0)}$,

$$\begin{aligned}
h_e(x_1, x_3, b_1, b_3) &= K_0\left(\sqrt{x_1 x_3} m_{B_s} b_1\right) \left[\theta(b_1 - b_3) K_0\left(\sqrt{x_3} m_{B_s} b_1\right) I_0\left(\sqrt{x_3} m_{B_s} b_3\right)\right. \\
&\left. + \theta(b_3 - b_1) K_0\left(\sqrt{x_3} m_{B_s} b_3\right) I_0\left(\sqrt{x_3} m_{B_s} b_1\right)\right] S_t(x_3),
\end{aligned} \tag{A1}$$

$$\begin{aligned}
h_a(x_2, x_3, b_2, b_3) &= K_0\left(i\sqrt{x_2 x_3} m_{B_s} b_2\right) \left[\theta(b_3 - b_2) K_0\left(i\sqrt{x_3} m_{B_s} b_3\right) I_0\left(i\sqrt{x_3} m_{B_s} b_2\right)\right. \\
&\left. + \theta(b_2 - b_3) K_0\left(i\sqrt{x_3} m_{B_s} b_2\right) I_0\left(i\sqrt{x_3} m_{B_s} b_3\right)\right] S_t(x_3),
\end{aligned} \tag{A2}$$

$$\begin{aligned}
h_f(x_1, x_2, x_3, b_1, b_2) &= \left\{\theta(b_2 - b_1) \mathrm{I}_0(M_{B_s}\sqrt{x_1 x_3} b_1) \mathrm{K}_0(M_{B_s}\sqrt{x_1 x_3} b_2)\right. \\
&\left. + (b_1 \leftrightarrow b_2)\right\} \cdot \begin{pmatrix} \mathrm{K}_0(M_{B_s} F_{(1)} b_2), & \text{for} \quad F_{(1)}^2 > 0 \\ \frac{\pi i}{2} \mathrm{H}_0^{(1)}(M_{B_s}\sqrt{|F_{(1)}^2|}\, b_2), & \text{for} \quad F_{(1)}^2 < 0 \end{pmatrix},
\end{aligned} \tag{A3}$$

$$\begin{aligned}
h_f^1(x_1, x_2, x_3, b_1, b_2) &= \left\{\theta(b_1 - b_2) \mathrm{K}_0(i\sqrt{x_2 x_3} b_1 M_{B_s}) \mathrm{I}_0(i\sqrt{x_2 x_3} b_2 M_{B_s})\right. \\
&\left. + (b_1 \leftrightarrow b_2)\right\} \cdot \begin{pmatrix} \mathrm{K}_0(M_{B_s} F_{(2)} b_1), & \text{for} \quad F_{(2)}^2 > 0 \\ \frac{\pi i}{2} \mathrm{H}_0^{(1)}(M_{B_s}\sqrt{|F_{(2)}^2|}\, b_1), & \text{for} \quad F_{(2)}^2 < 0 \end{pmatrix},
\end{aligned} \tag{A4}$$

$$\begin{aligned}
h_f^2(x_1, x_2, x_3, b_1, b_2) &= \left\{\theta(b_1 - b_2) \mathrm{K}_0(i\sqrt{x_2 x_3} b_1 M_{B_s}) \mathrm{I}_0(i\sqrt{x_2 x_3} b_2 M_{B_s})\right. \\
&\left. + (b_1 \leftrightarrow b_2)\right\} \cdot \begin{pmatrix} \mathrm{K}_0(M_{B_s} F_{(3)} b_1), & \text{for} \quad F_{(3)}^2 > 0 \\ \frac{\pi i}{2} \mathrm{H}_0^{(1)}(M_{B_s}\sqrt{|F_{(3)}^2|}\, b_1), & \text{for} \quad F_{(3)}^2 < 0 \end{pmatrix},
\end{aligned} \tag{A5}$$

where J_0 is the Bessel function, K_0 and I_0 are modified Bessel functions $K_0(-ix) = -(\pi/2)Y_0(x) + i(\pi/2)J_0(x)$; $\mathrm{H}_0^{(1)}(z)$ is the Hankel function ,$\mathrm{H}_0^{(1)}(z) = \mathrm{J}_0(z) + i\,\mathrm{Y}_0(z)$, and $F_{(j)}$'s are defined by

$$\begin{aligned} F_{(1)}^2 &= (x_1 - x_2)x_3\ , \\ F_{(2)}^2 &= (x_1 - x_2)x_3\ , \\ F_{(3)}^2 &= x_1 + x_2 + x_3 - x_1x_3 - x_2x_3\ . \end{aligned} \tag{A6}$$

The threshold resummation form factor $S_t(x_i)$ is adopted from Ref.[24]

$$S_t(x) = \frac{2^{1+2c}\Gamma(3/2+c)}{\sqrt{\pi}\Gamma(1+c)}[x(1-x)]^c, \tag{A7}$$

where the parameter $c = 0.3$. This function is normalized to unity. More information about the threshold resummation can be found in reference [19].

The Sudakov factors used in the text are defined as

$$\begin{aligned} S_{ab}(t) &= s\left(x_1 m_{B_s}/\sqrt{2}, b_1\right) + s\left(x_3 m_{B_s}/\sqrt{2}, b_3\right) + s\left((1-x_3) m_{B_s}/\sqrt{2}, b_3\right) \\ &\quad -\frac{1}{\beta_1}\left[\ln\frac{\ln(t/\Lambda)}{-\ln(b_1\Lambda)} + \ln\frac{\ln(t/\Lambda)}{-\ln(b_3\Lambda)}\right], \end{aligned} \tag{A8}$$

$$\begin{aligned} S_{cd}(t) &= s\left(x_1 m_{B_s}/\sqrt{2}, b_1\right) + s\left(x_2 m_{B_s}/\sqrt{2}, b_2\right) + s\left((1-x_2) m_{B_s}/\sqrt{2}, b_2\right) \\ &\quad + s\left(x_3 m_{B_s}/\sqrt{2}, b_1\right) + s\left((1-x_3) m_{B_s}/\sqrt{2}, b_1\right) \\ &\quad -\frac{1}{\beta_1}\left[2\ln\frac{\ln(t/\Lambda)}{-\ln(b_1\Lambda)} + \ln\frac{\ln(t/\Lambda)}{-\ln(b_2\Lambda)}\right], \end{aligned} \tag{A9}$$

$$\begin{aligned} S_{ef}(t) &= s\left(x_1 m_{B_s}/\sqrt{2}, b_1\right) + s\left(x_2 m_{B_s}/\sqrt{2}, b_2\right) + s\left((1-x_2) m_{B_s}/\sqrt{2}, b_2\right) \\ &\quad + s\left(x_3 m_{B_s}/\sqrt{2}, b_2\right) + s\left((1-x_3) m_{B_s}/\sqrt{2}, b_2\right) \\ &\quad -\frac{1}{\beta_1}\left[\ln\frac{\ln(t/\Lambda)}{-\ln(b_1\Lambda)} + 2\ln\frac{\ln(t/\Lambda)}{-\ln(b_2\Lambda)}\right], \end{aligned} \tag{A10}$$

$$\begin{aligned} S_{gh}(t) &= s\left(x_2 m_{B_s}/\sqrt{2}, b_2\right) + s\left(x_3 m_{B_s}/\sqrt{2}, b_3\right) + s\left((1-x_2) m_{B_s}/\sqrt{2}, b_2\right) \\ &\quad + s\left((1-x_3) m_{B_s}/\sqrt{2}, b_3\right) - \frac{1}{\beta_1}\left[\ln\frac{\ln(t/\Lambda)}{-\ln(b_3\Lambda)} + \ln\frac{\ln(t/\Lambda)}{-\ln(b_2\Lambda)}\right], \end{aligned} \tag{A11}$$

where the function S_{B_s}, $S_{\rho(\omega)}$, S_K used in the amplitudes are defined as:

$$S_{B_s}(t) = s(x_1 P_1^+, b_1) + 2\int_{1/b_1}^{t} \frac{d\bar{\mu}}{\bar{\mu}}\gamma(\alpha_s(\bar{\mu})), \tag{A12}$$

$$S_{\rho(\omega)}(t) = s(x_2 P_2^+, b_2) + s\left((1-x_2)P_2^+, b_2\right) + 2\int_{1/b_2}^{t} \frac{d\bar{\mu}}{\bar{\mu}}\gamma\left(\alpha_s(\bar{\mu})\right), \tag{A13}$$

$$S_K(t) = s(x_3 P_3^-, b_3) + s\left((1-x_3)P_3^-, b_3\right) + 2\int_{1/b_3}^{t} \frac{d\bar{\mu}}{\bar{\mu}}\gamma\left(\alpha_s(\bar{\mu})\right). \tag{A14}$$

where the so called Sudakov factor $s(Q,b)$ resulting from the resummation of double logarithms is given as [32]:

$$s(Q,b) = \int_{1/b}^{Q} \frac{d\mu}{\mu} \Big[\ln\left(\frac{Q}{\mu}\right) A(\alpha(\bar{\mu})) + B(\alpha_s(\bar{\mu})) \Big] \tag{A15}$$

with

$$\begin{aligned} A &= C_F \frac{\alpha_s}{\pi} + \left[\frac{67}{9} - \frac{\pi^2}{3} - \frac{10}{27} n_f + \frac{2}{3}\beta_0 \ln\left(\frac{e^{\gamma_E}}{2}\right) \right] \left(\frac{\alpha_s}{\pi}\right)^2 , \\ B &= \frac{2}{3}\frac{\alpha_s}{\pi} \ln\left(\frac{e^{2\gamma_E - 1}}{2}\right) . \end{aligned} \tag{A16}$$

Here $\gamma_E = 0.57722\cdots$ is the Euler constant, n_f is the active quark flavor number.

The hard scale t_i's in the above equations are chosen as:

$$\begin{aligned} t_e^1 &= \max(\sqrt{x_3} m_{B_s}, 1/b_1, 1/b_3) , \\ t_e^2 &= \max(\sqrt{x_1} m_{B_s}, 1/b_1, 1/b_3) , \\ t_e^3 &= \max(\sqrt{x_3} m_{B_s}, 1/b_2, 1/b_3) , \\ t_e^4 &= \max(\sqrt{x_2} m_{B_s}, 1/b_2, 1/b_3) , \\ t_f &= \max(\sqrt{x_1 x_3} m_{B_s}, \sqrt{x_2 x_3} m_{B_s}, 1/b_1, 1/b_2) , \\ t_f^1 &= \max(\sqrt{x_2 x_3} m_{B_s}, 1/b_1, 1/b_2) , \\ t_f^2 &= \max(\sqrt{x_1 + x_2 + x_3 - x_1 x_3 - x_2 x_3} m_{B_s}, \sqrt{x_2 x_3} m_{B_s}, 1/b_1, 1/b_2) . \end{aligned} \tag{A17}$$

They are given as the maximum energy scale appearing in each diagram to kill the large logarithmic radiative corrections.

---

[1] P. Ball *et al.*, CERN Yellow Report 2000-004; hep-ph/0003238.

[2] S. Stone, talk given at the Aspen Winter Conference, Aspen, Colorado, USA; February, 2006; G. Raven, talk given at the Belle-ITEP Meeting on the Future of Heavy Flavour Physics, ITEP Moscow, Russian, July 24-25, 2006; T. Ruf, talk given at the XXXIII International Conference on High Energy Physics (ICHEP'06), Moscow, Russian, July 26-August 2, 2006.

[3] M. Wirbel, B. Stech, and M. Bauer, Z. Phys. C **29**, 637 (1985); M. Bauer, B. Stech, and M. Wirbel, Z. Phys. C **34**, 103 (1987).

[4] A. Ali, G. Kramer and C.D. Lü, Phys. Rev. D **58**, 094009 (1998); *ibid.* **59**, 014005 (1999);

[5] Y.-H. Chen, H.Y. Cheng, B. Tseng, and K.C. Yang, Phys. Rev. D **60**, 094014 (1999); H.Y. Cheng and K.C. Yang, Phys. Rev. D **62**, 054029 (2000).

[6] M. Beneke, G. Buchalla, M. Neubert and C.T. Sachrajda, Phys. Rev. Lett. 83, 1914 (1999); Nucl. Phys. B **591**, 313 (2000).

[7] Y.H. Chen, H.Y. Cheng, B. Tseng, Phys. Rev. D **59**, 074003 (1999).

[8] B. Tseng, Phys. Lett. B **446**, 125 (1999).

[9] J.F. Sun, G.H. Zhu, D.S. Du, Phys. Rev. D **68**, 054003 (2003).

[10] M. Beneke and M. Neubert, Nucl. Phys. B **675**, 333 (2003).

[11] D. Zhang, Z.J. Xiao, and C.S. Li, Phys. Rev. D **64**, 014014 (2001).
[12] Y. Li, C.D. Lü, Z.J. Xiao, and X.Q. Yu, Phys. Rev. D **70**, 034009 (2004).
[13] X.Q. Yu, Y. Li and C.D. Lü, Phys. Rev. D **73**, 017501 (2006).
[14] X.Q. Yu, Y. Li, and C.D. Lü, Phys. Rev. D **71**, 074026 (2005).
[15] J. Zhu, Y.L. Shen, and C.D. Lü, J. Phys. G **32**, 101 (2006).
[16] Z.J. Xiao, X. Liu and H.S. Wang, hep-ex/0606177.
[17] H.N. Li and H.L. Yu, Phys. Rev. Lett. **74**, 4388 (1995); Phys. Lett. B **353**, 301 (1995); C.H. Chang and H.N. Li, Phys. Rev. D **55**, 5577 (1997); T.W. Yeh and H.N. Li, Phys. Rev. D **56**, 1615 (1997).
[18] Y.-Y. Keum, H.N. Li, and A.I. Sanda, Phys. Lett. B **504**, 6 (2001); Phys. Rev. D **63**, 054008 (2001).
[19] H.N. Li, Phys. Rev. D **66**, 094010 (2002).
[20] H.N. Li and B. Tseng, Phys. Rev. D **57**, 443 (1998).
[21] G. Buchalla, A.J. Buras, M.E. Lautenbacher, Rev. Mod. Phys. **68**, 1125 (1996).
[22] C.D. Lü, K. Ukai, and M.Z. Yang, Phys. Rev. D **63**, 074009 (2001).
[23] A.G. Grozin and M. Neubert, Phys. Rev. D **55**, 272 (1997); M. Beneke and T. Feldmann, Nucl. Phys. B **592**, 3 (2001).
[24] T. Kurimoto, H.N. Li, and A.I. Sanda, Phys. Rev. D **65**, 014007 (2002); C.D. Lu and M.Z. Yang, Eur. Phys. J. C **28**, 515 (2003).
[25] P. Ball, V.M. Braun, Y. Koike, and K. Tanaka, Nucl. Phys. B **529**, 323 (1998)
[26] Particle Data Group, S. Eidelman *et al.*, Phys. Lett. B **592**, 1 (2004).
[27] X.Q. Li, G.R. Lu, and Y.D. Yang, Phys. Rev. D **68**, 114015 (2003).
[28] A. Khodjamirian, T. Mannel and M. Melcher, Phys. Rev. D **70**, 094002 (2004); V.M. Braun and A. Lenz, Phys. Rev. D **70**, 074020 (2004).
[29] V.M. Braun and I.E. Filyanov , Z. Phys. C **48**, 239 (1990); P. Ball, J. High Energy Phys. **01**, 010 (1999).
[30] D.S. Du and Z.Z. Xing, Phys. Rev. D **48**, 3400 (1993); D.S. Du and M.Z. Yang, Phys. Lett. B **358**, 123 (1995).
[31] H.N. Li, S. Mishima, A.I. Sanda, Phys. Rev. D **72**, 114005 (2005).
[32] H.N. Li and B. Melic, Eur. Phys. J. C **11**, 695(1999); H.N. Li and K. Ukai, Phys. Lett. B **555**, 197 (2003).